

Effect of Hydrogen Pick-up and Release Behavior on the Tensile Properties of Electroplated 4340M High-strength Steel

A Senior Project
presented to
the Faculty of the Materials Engineering Department
California Polytechnic State University, San Luis Obispo

In Partial Fulfillment
of the Requirements for the Degree
Bachelor of Science, Materials Engineering

Blake Daylor, Josh Fisher, Alan Michelen Ruiz
Advisor: Prof. Blair London
Sponsor: The Boeing Company

June 6, 2016

Abstract

Hydrogen embrittlement of high-strength steel (4340M) was quantified through tensile testing and fractography (SEM). Three types of samples were obtained: rotating beam fatigue specimens, round (notched) tensile specimens, and flat panel specimens. In addition, three different plating types were analyzed (Ni, Cr, Cd-Ti) with a set of samples that was shot peened and a set that was not. Since some of the samples went through a hydrogen relief bake, another factor in our experiment was the amount of time it took for the samples to reach the baking process after they were electroplated (bake delay). There were three levels of bake delay that were studied for each type of plating: specified bake, delayed bake, and no bake. The notched tensile specimens and the rotating beam specimens were tensile tested, and their fracture surfaces were imaged and analyzed. The flat panel specimens were notched and manually fractured in a vise, and fractography was performed to characterize failure modes. To determine the amount of hydrogen input and release from the various samples, LECO combustion analysis was performed. The hydrogen content was used to correlate the various processing conditions (electroplating type, shot peening, bake delay) to their tensile properties and failure modes.

Key Words: Hydrogen, hydrogen embrittlement, hydrogen pick-up, 4340M steel, landing gears, shot peening, electroplating, hydrogen relief bake, bake delay, high-strength steel, nickel, chromium, cadmium-titanium, laboratory fracture, materials engineering

Acknowledgements

We would like to thank The Boeing Company for sponsoring this project, and especially our industry contacts Craig Dickerson and Bob Weiss. We appreciate the opportunity and the help received throughout the process of completing this project. We would also like to thank the Materials Engineering department for allowing us to utilize their equipment and facilities. We would also like to thank Luka Dugandzic for manufacturing the attachments for the button head fixture and Wyoming Test Fixtures for providing this fixture. Lastly, we would like to thank Professor Blair London, our senior project advisor, for his support and guidance in completing the project.

Table of Contents

| | |
|--|----|
| 1. Problem Statement | 1 |
| 2. Background | 1 |
| 2.1. Landing Gear | 1 |
| 2.2. Processing | 2 |
| 2.2.1. Shot Peening..... | 2 |
| 2.2.2. Electroplating | 4 |
| 2.2.2.1. Types and Functions of Electroplating..... | 5 |
| 3. Effects of Processes on Hydrogen Pick-up..... | 6 |
| 3.1. Hydrogen Pick-up | 6 |
| 3.1.1. Effects of Electroplating Process on Hydrogen Pick-up | 7 |
| 3.1.2. Effects of Shot Peening Process on Hydrogen Pick-up..... | 9 |
| 4. Effects of Hydrogen Pick-up on 4340M High-strength Steel..... | 9 |
| 4.1. Hydrogen Embrittlement..... | 9 |
| 4.2. Failure Modes..... | 10 |
| 4.3. Hydrogen Relief Bake..... | 12 |
| 4.4. Stress Relief Bake | 13 |
| 5. Experimental Procedure..... | 14 |
| 5.1. Safety..... | 14 |
| 5.2. Samples | 15 |
| 5.2.1. Sample Types | 15 |
| 5.2.2. Material Variation..... | 16 |
| 5.2.3. Sample Preparation..... | 17 |
| 5.3. Sample Processing..... | 17 |
| 5.3.1. Shot Peening | 17 |
| 5.3.2. Electroplating..... | 17 |
| 5.3.3. Hydrogen Relief Bake | 18 |
| 5.4. Metallography | 19 |
| 5.5. Testing..... | 19 |
| 5.5.1. Tensile Testing | 20 |
| 5.5.2. Laboratory Fractures..... | 21 |

| | |
|---|----|
| 5.6. Fracture Surface Analysis | 22 |
| 6. Results..... | 22 |
| 6.1. Residual Stress Measurements..... | 22 |
| 6.2. Metallography | 24 |
| 6.3. Hydrogen Relief | 25 |
| 6.4. Hydrogen Pick-up | 25 |
| 6.5. Tensile Testing Results | 28 |
| 6.6. Fracture Analysis..... | 30 |
| 6.6.1. Non-shot Peened Flat Panels | 31 |
| 6.6.2. Shot Peened Flat Panels..... | 32 |
| 7. Discussion..... | 33 |
| 7.1. Baking Efficiency..... | 33 |
| 7.2. Effect of Shot Peening on Hydrogen Pick-up | 33 |
| 7.3. Effect of Bake Delay on Hydrogen Pick-up..... | 34 |
| 7.4. Effect of Bake Delay on Hydrogen Embrittlement..... | 34 |
| 7.5. Effect of Electroplating on Hydrogen Embrittlement | 35 |
| 8. Conclusions..... | 35 |
| 9. References..... | 36 |

List of Figures

FIGURE 1. PROCESS OVERVIEW OF 4340M STRUCTURAL MEMBERS FOR BOEING LANDING GEAR.....2

FIGURE 2. THIS IMAGE SHOWS THE MECHANICAL YIELDING OF THE MATERIAL AT THE POINT OF IMPACT OF THE SHOT PEENING MEDIA. FURTHERMORE, THE MEDIA PRODUCES A COMPRESSIVE LAYER THAT INCREASES THE RESISTANCE TO FATIGUE CRACKING.3

FIGURE 3. CRACK INITIATION AND GROWTH THROUGH TENSILE STRESS.....3

FIGURE 4. THIS FIGURE ILLUSTRATES THE CONCEPT OF ELECTROPLATING AND SERVES AS A VISUAL REPRESENTATION FOR THE DEPOSITION PROCESS. CURRENT IS DRIVEN THROUGH THE ANODE WHICH FORCES THE RELEASE OF NEGATIVE IONS INTO THE ELECTROLYTE SOLUTION THAT REDUCE AT THE CATHODE-ELECTROLYTE INTERFACE AND ATTACH ONTO IT (PLATING).4

FIGURE 5. SHOWS PREFERRED LOCATIONS OF HYDROGEN IN THE LATTICE.....7

FIGURE 6. HYDROGEN PENETRATION CURRENT VERSUS TIME IN A NON-CYANIDE ELECTROLYTE SOLUTION FOR CADMIUM PLATING WITH VARYING TITANIUM CONCENTRATIONS: (1) NO TI, (2) 0.067 G/L TI, (3) 2.2 G/L TI, (4) 3.1 G/L TI.....8

FIGURE 7. THE ILLUSTRATION AND MICROGRAPH ON THE LEFT REPRESENT TRANSGRANULAR FRACTURE. ON THE RIGHT ARE EXAMPLES OF INTERGRANULAR FRACTURE.11

FIGURE 8. BRITTLE FAILURE OF CADMIUM PLATED STEEL NUT.....11

FIGURE 9. THE TEST SETUP FOR THE NOTCHED TENSILE SAMPLES IS SHOWN. THE SAMPLES WERE INSERTED IN THE BUTTON HEAD FIXTURES AND PULLED AT A RATE OF 0.1 IN./MIN.20

FIGURE 10. ROTATING BEAM SPECIMEN AFTER TENSILE TEST IS SHOWN. NOTE THAT THE SAMPLE WAS TESTED AT A CROSSHEAD RATE OF 0.2 IN./MIN.21

FIGURE 11. THIS IMAGE SHOWS THE FLAT PANEL SPECIMENS THAT WERE CUT OUT INTO THE LAB FRACTURE SAMPLES, THE NOTCHES, AND THE FINAL SAMPLE SURFACES. THE SAMPLES USED FOR THE LAB FRACTURES HAD DIMENSIONS OF ROUGHLY 1.5 IN. X 0.5 IN. X 0.25 IN.....22

FIGURE 12. RESIDUAL STRESS FOR TWO NON-SHOT PEENED, FLAT PANEL SPECIMENS DEMONSTRATING PRIMARILY TENSILE (POSITIVE) STRESSES NEAR THE SURFACE WITH SMALL COMPRESSIVE (NEGATIVE) STRESSES UP TO 0.004" (A) AND 0.005" (B) INTO THE SURFACE DUE TO ABRASIVE BLASTING.23

FIGURE 13. RESIDUAL STRESS FOR TWO SHOT PEENED, FLAT PANEL SPECIMENS DEMONSTRATING PRIMARILY COMPRESSIVE (NEGATIVE) STRESSES UP TO 0.012" (A) AND 0.005" (B) INTO THE SURFACE DUE TO SHOT PEENING.24

FIGURE 14. THESE IMAGES SHOW THE MICROSTRUCTURES OF THE THREE PLATINGS. NOTICE THE POROSITY OF THE CD-TI PLATING, AND THE DENSITY AND COMPACTNESS OF THE NI AND CR ONES. IN ADDITION, THE NOTE THAT THE CR PLATING SUFFERS FROM MICROCRACKING.24

FIGURE 15. THIS BAR CHART FURTHER SHOWS THE EFFECTS OF THE HYDROGEN RELIEF BAKE DELAY SPECIFICATIONS ON THE HYDROGEN CONTENT OF THE SAMPLE. NOTE THAT AS BAKE DELAY INCREASES, HYDROGEN PICK-UP INCREASES.28

FIGURE 16. THIS FIGURE SHOWS THE AVERAGE MAXIMUM STRESSES OF THE SAMPLES IN THE "AS RECEIVED" CONDITION (BASELINE), THE SHOT PEENED SAMPLES IN THE "SPECIFIED BAKE" CONDITION, AND THE SHOT PEENED SAMPLES IN THE "NO BAKE" CONDITION. THESE ARE THE ROTATING FATIGUE BEAM SPECIMENS WHICH MEANS THAT THE MATERIAL IS 4330M STEEL IN THE 200-220 KSI RANGE. THIS FIGURE SHOWS THE FACT THAT ELECTROPLATING DOES IN FACT EMBRITTLE THE MATERIAL, LOWERING ϵ_{MAX} . IN ADDITION, THERE IS A SIGNIFICANT DIFFERENCE BETWEEN SAMPLES THAT ARE BAKED, AND SAMPLES THAT ARE NOT, WHERE THE BAKED SAMPLES HAVE A MUCH HIGHER MAXIMUM STRESS.29

FIGURE 17. THIS FIGURE SHOWS THE AVERAGE MAXIMUM STRESSES OF THE SAMPLES IN THE "AS RECEIVED" CONDITION (BASELINE), THE NON-SHOT PEENED SAMPLES IN THE "SPECIFIED BAKE" CONDITION, AND THE NON-SHOT PEENED SAMPLES IN THE "NO BAKE" CONDITION. THESE ARE THE NOTCHED TENSILE SAMPLES WHICH MEANS THAT THE MATERIAL IS 4340 STEEL IN THE 275-300 KSI STRENGTH RANGE. THE STRESS CONCENTRATION

FACTOR OF THE NOTCH WAS NOT INCLUDED IN THE CALCULATIONS, HOWEVER A RELATIVE COMPARISON OF THE VALUES IS STILL VALID. NOTICE THAT ELECTROPLATING DOES IN FACT EMBRITTLE THE MATERIAL, LOWERING EMAX. IN ADDITION, THERE IS A SIGNIFICANT DIFFERENCE BETWEEN SAMPLES THAT ARE BAKED, AND SAMPLES THAT ARE NOT, WHERE THE BAKED SAMPLES HAVE A MUCH HIGHER MAXIMUM STRESS.30

FIGURE 18. SCANNING ELECTRON MICROSCOPE FRACTOGRAPHS (2500X MAGNIFICATION) OF NON-SHOT PEENED, NICKEL PANEL SPECIMENS WITH INCREASING BAKE DELAY: (A) SPECIFIED BAKE (B) DELAYED BAKE (C) NO BAKE. AS BAKE DELAY INCREASE, THE PROMINENCE OF BRITTLE FACETS INCREASES AND THE DUCTILE DIMPLE REGIONS DECREASE.31

FIGURE 19. SCANNING ELECTRON MICROSCOPE FRACTOGRAPHS (2500X MAGNIFICATION) OF NON-SHOT PEENED, HARD CHROMIUM PANEL SPECIMENS WITH INCREASING BAKE DELAY: (A) SPECIFIED BAKE (B) DELAYED BAKE (C) NO BAKE. AS BAKE DELAY INCREASE, THE PROMINENCE OF BRITTLE FACETS INCREASES AND THE DUCTILE DIMPLE REGIONS DECREASE.31

FIGURE 20. SCANNING ELECTRON MICROSCOPE FRACTOGRAPHS (2500X MAGNIFICATION) OF NON-SHOT PEENED, CADMIUM-TITANIUM PANEL SPECIMENS WITH INCREASING BAKE DELAY: (A) SPECIFIED BAKE (B) DELAYED BAKE (C) NO BAKE. AS BAKE DELAY INCREASE, THE PROMINENCE OF BRITTLE FACETS INCREASES AND THE DUCTILE DIMPLE REGIONS DECREASE.31

FIGURE 21. SCANNING ELECTRON MICROSCOPE FRACTOGRAPHS (2500X MAGNIFICATION) OF SHOT PEENED, NICKEL PANEL SPECIMENS WITH INCREASING BAKE DELAY: (A) SPECIFIED BAKE (B) DELAYED BAKE (C) NO BAKE. ALL THE IMAGES APPEAR TO BE PRIMARILY DUCTILE BUT AS BAKE DELAY INCREASE, THE PROMINENCE OF BRITTLE FACETS INCREASES AND THE DUCTILE DIMPLE REGIONS DECREASE.32

FIGURE 22. SCANNING ELECTRON MICROSCOPE FRACTOGRAPHS (2500X MAGNIFICATION) OF SHOT PEENED, HARD CHROMIUM PANEL SPECIMENS WITH INCREASING BAKE DELAY: (A) SPECIFIED BAKE (B) DELAYED BAKE (C) NO BAKE. ALL THE IMAGES APPEAR TO BE PRIMARILY DUCTILE BUT AS BAKE DELAY INCREASE, THE PROMINENCE OF BRITTLE FACETS INCREASES AND THE DUCTILE DIMPLE REGIONS DECREASE.32

FIGURE 23. SCANNING ELECTRON MICROSCOPE FRACTOGRAPHS (2500X MAGNIFICATION) OF SHOT PEENED, HARD CHROMIUM PANEL SPECIMENS WITH INCREASING BAKE DELAY: (A) SPECIFIED BAKE (B) DELAYED BAKE (C) NO BAKE. ALL THE IMAGES APPEAR TO BE PRIMARILY DUCTILE BUT AS BAKE DELAY INCREASE, THE PROMINENCE OF BRITTLE FACETS INCREASES AND THE DUCTILE DIMPLE REGIONS DECREASE.32

List of Tables

TABLE I. HYDROGEN CONCENTRATION ANALYSIS OF CADMIUM PLATED 4340 STEEL WITH VARYING HYDROGEN RELIEF BAKE AND BAKE DELAY TIMES9

TABLE II. BOEING SPECIFICATIONS FOR HYDROGEN RELIEF BAKING OF CHROMIUM, NICKEL, AND CADMIUM-TITANIUM 300M STEEL AT A BAKE TEMPERATURE OF 375°F13

TABLE III. SAMPLE TYPES AND PROCESSING SPECIFICATIONS16

TABLE IV. BAKE DELAY TIMES FOR NOTCHED TENSILE SPECIMENS AND FATIGUE COUPONS18

TABLE V. BAKE DELAY TIMES FOR PANEL SPECIMENS.....19

TABLE VI. BAKE OUT EFFICIENCY25

TABLE VII. SHOT PEENING EFFECTS ON HYDROGEN PICK-UP.....26

TABLE VIII. NORMALIZED HYDROGEN CONTENT FOR THE FLAT PANEL SPECIMENS.....27

TABLE IX. MECHANICAL PROPERTIES OF ROTATING BEAM FATIGUE SPECIMENS28

TABLE X. MECHANICAL PROPERTIES OF NOTCHED TENSILE SAMPLES29

1. Problem Statement

The purpose of this project is to investigate the effects of hydrogen pick-up and release on electroplated 4340M steel. Hydrogen degrades metallic materials by cracking, blistering, hydride formation, decarburization, and lowers both tensile strength and ductility. High strength steel such as 4340M is susceptible to even minimal amounts of hydrogen pick-up. Literature has shown that shot peening, electroplating, and bake delay (time between electroplating and hydrogen relief bake) affect hydrogen pick-up. To determine the influence of these factors on hydrogen pick-up, three different types of electroplating were tested: nickel, chromium, and cadmium-titanium. For each coating, both shot peened and non-shot peened samples with various bake delays were tested to investigate their effects on hydrogen pick-up and embrittlement. The Boeing Company (Everett, WA) directly measured hydrogen pick-up, SEM and metallography was performed in the MatE Department, together with notched tensile testing and tensile testing of the rotating beam specimens. These tests allowed the investigation of hydrogen embrittlement in the samples, as well as its failure modes. The flat panel specimens were notched and manually fractured in a vise, and fractography was performed to characterize failure modes. The goal was to have conclusive and new data on how shot peening, electroplating, and bake delay affect hydrogen pick-up and the resulting properties of the steel.

2. Background

2.1. Landing Gear

The main purpose of aircraft landing gear is to support the entire weight of an aircraft during landing and ground operations. They are attached to important structural members of the aircraft. There are different types of gears depending on the aircraft design and its intended use. Landing gears have wheels to facilitate operation to and from hard surfaces, such as airport runways. There is a whole system included in the mechanics and design of landing gear regardless of the type of landing gear utilized. This system includes parts that are necessary to attach the gear to the aircraft. Examples of these are shock absorbing equipment, brakes, retraction mechanisms, controls, warning devices, cowling, fairings, and structural members. [1]

2.2. Processing

Boeing has a general manufacturing flow for all 4340M parts manufactured for structural applications in their landing gear department. The typical overall processing flow for their parts is shown in Figure 1.

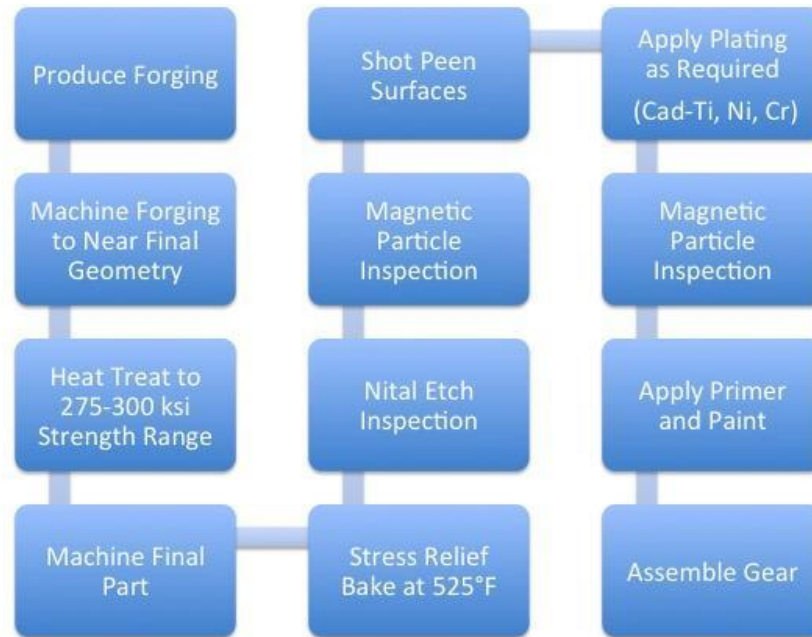


Figure 1. Process overview of 4340M structural members for Boeing landing gear. [2]

2.2.1. Shot Peening

Shot peening is a cold working process in which the surface of a part is bombarded with small spherical media called shot. Each shot that strikes the metal acts as a “tiny peening hammer” resulting in a small surface indentation (Figure 2a). In order for the indentation to be formed, the surface layer of the metal must yield in tension (Figure 2b). Below the surface, the compressed grains attempt to restore the surface to its original shape producing a hemisphere of cold-worked metal highly stressed in compression (Figure 2b). Overlapping dimples develop a uniform layer of residual compressive stress. [3]

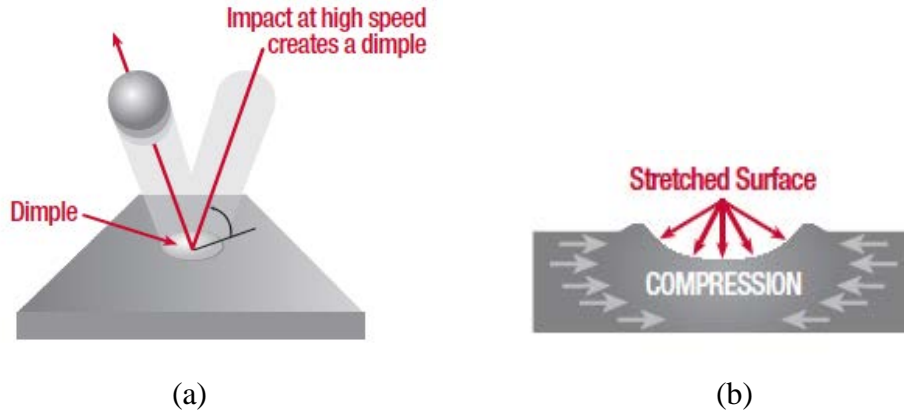


Figure 2. This image shows the mechanical yielding of the material at the point of impact of the shot peening media. Furthermore, the media produces a compressive layer that increases the resistance to fatigue cracking. [3]

Cracks will not initiate nor propagate in a compressively stressed zone. Because nearly all fatigue and stress corrosion failures originate at or near the surface of a part, surface compressive stress provides a significant increase in part life. The magnitude of residual compressive stress produced by shot peening is at least as great as half the tensile strength of the material being peened. [3]

In most modes of long term failure the common factor is tensile stress. These stresses can either result from externally applied loads, or stem from manufacturing processes such as welding, grinding or machining. Tensile stresses attempt to stretch or pull the surface apart and may eventually lead to crack initiation (Figure 3). Compressive stresses constrict the bonds between atoms in the lattice and will significantly delay the initiation of fatigue cracking. Because crack growth is slowed significantly in a compressive layer, increasing the depth of this layer increases crack resistance. Shot peening is the most economical and practical method of ensuring surface residual compressive stresses. [3]

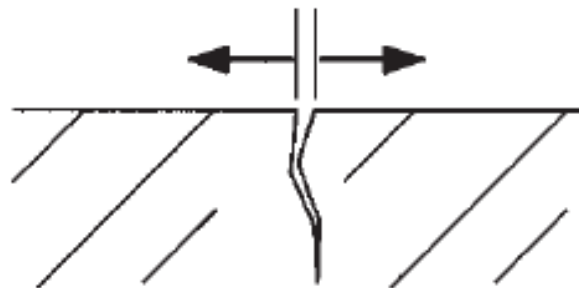


Figure 3. Crack initiation and growth through tensile stress.

2.2.2. Electroplating

Electrodeposition or electroplating is defined as the process in which a coating is deposited by electrolysis, that is, a metal is deposited on an electrode immersed in an electrolyte by passing electric current through the electrolyte. [4] This process is similar to a galvanic corrosion cell, except the current moves the opposite direction. The cathode (i.e. steel) is plated, and the anode is the metal to be plated on the component. The anode and cathode are submerged in the electrolyte solution, which contains metal salts and other ions which produces electrical conductivity. The anode is supplied with a current which oxidizes its metal atoms dissolving them in the solution. The metal atoms that lie in the electrolyte are then reduced when they come in contact with the cathode and are deposited onto it. A simple representation of the process is shown in Figure 4. The rate of this process is proportional to the current that runs through the system, which dissolves the ions from the anode into the electrolyte and drives the process.

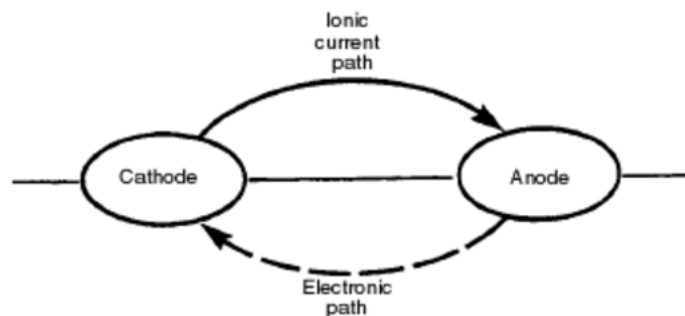


Figure 4. This figure illustrates the concept of electroplating and serves as a visual representation for the deposition process. Current is driven through the anode which forces the release of negative ions into the electrolyte solution that reduce at the cathode-electrolyte interface and attach onto it (plating). [5]

Electroplated coatings are applied to steel for corrosion resistance, appearance, solderability, or other special requirements. A wide variety of materials are electroplated on steel, including nickel, chromium, zinc, cadmium, and tin. Multilayer coatings can also be applied by electroplating; an example is the copper-nickel-chromium plating system used for bright automotive trim or cadmium-titanium for landing gear components. [6]

As with every process, electroplating has drawbacks. These include the inability to achieve a uniform deposition. This is because of a phenomenon called throwing power. This phenomenon is dependent on the shape of the substrate (cathode), the current density of the system, as well as the composition and conductivity of the electrolyte. In addition, it must be mentioned that not all

metallic elements can be deposited. In order for proper plating, all surface contaminants must also be eliminated to ensure adhesion and surface quality. Good adhesion relies on both the elimination of surface contaminants (to produce a good metallurgical bond) and the generation of a completely active surface to initiate plating on all areas. Substrate preparation includes rough cleaning, alkaline cleaning, electrocleaning, acid treatments, and other cleaning processes. Good bonds can be achieved, however they can never be as good as a fusion bonds. Poor bonds are threatening to the essence of the product, because they cannot be detected easily.

There are several advantages to using the electroplating process to produce a coating, including the fact that the component will remain metallurgically intact (temperature will not exceed 100°C or 212°F so microstructures will not be affected). However, the plating process can be adjusted to manipulate the hardness, internal stress, and metallurgical properties of the coating. In addition, electroplating allows for a dense and tightly adhered coating whose thickness can be controlled by the current density and length of time of the deposition. Furthermore, plating rates can be accelerated through electrolyte circulation. Technical limits for thickness of coating and size of components are only confined to the size of the bath tank, and specific areas can be protected from coating by utilizing masks. The process overall is appropriate for automation and seems to surpass other coating processes economically.

2.2.2.1. Types and Functions of Electroplating

2.2.2.1.1. Cadmium-Titanium Plating

Cadmium-titanium is the primary alloy plating type Boeing uses on all 4340M landing gear parts. Boeing uses a cadmium-titanium alloy containing between 0.1 and 0.7 wt% titanium. Per Standard BAC5804, cadmium-titanium plating is intended for use on low alloy and corrosion resistant steels, including steels heat treated to strength levels above 220 ksi. [7] The corrosion resistance results due to the more anodic tendency of cadmium compared to iron. The underlying steel is protected at the expense of the corroding cadmium plate even with the presence of scratches in the coating. [8] To protect from atmospheric corrosion, cadmium is applied as a thin layer (less than 25 μm or 1000 $\mu\text{in.}$ thick). One of the primary advantages of cadmium plating over other plating types is the ductility which allows coated steel to be formed and

shaped. Cadmium is also highly toxic, which is driving concerns to reduce and eliminate its use in many applications. [8]

2.2.2.1.2. Hard Chromium Plating

Hard chromium plating is used for applications requiring excellent wear and corrosion resistance. The surface of hard chromium plating provides a low coefficient of friction that resists corrosion, galling, and abrasive and lubricated wear. Hard chromium plating is produced by electrodeposition from a solution containing chromic acid (CrO_3) and a catalytic anion. The deposited layer typically ranges in thickness from 2.5 to 500 μm . The major applications of hard chromium include improvement of tool performances, tool life, and part salvage. Other applications include piston rings, aircraft landing gear, textile and gravure rolls. [9]

2.2.2.1.3. Electrodeposited Nickel Plating

Nickel plating is performed in engineering applications to enhance a variety of properties, and these depend on the composition of the plating bath and operating conditions. Most of these properties are surface properties, such as corrosion resistance, hardness, wear, and magnetic properties. [10] General-purpose nickel is mainly utilized to protect steels against corrosive attack in rural, marine, and industrial atmospheres. In addition, nickel plating is used for decorative purposes. Bright nickel plating can be combined with a lower layer of sulfur-free, semi-bright nickel and thinner upper layer of chromium that provide a bright corrosion-resistant finish and wear-resistant surface to steel. Applications for these types of coatings are decorative trim for automotive and consumer products. [6]

3. Effects of Processes on Hydrogen Pick-up

3.1. Hydrogen Pick-up

There is still much unknown about hydrogen pickup with regards to the nature of the equilibrium absorption site, why hydrogen has preferred interstitial locations, and how to deal with diffusion barriers. What is known is that there are two common locations for hydrogen in the BCC structure of iron, tetrahedral sites (T-sites) and octahedral sites (O-sites) (Figure 5). While this is not universal for all circumstances, T-sites seem to be more common of the two. [11]

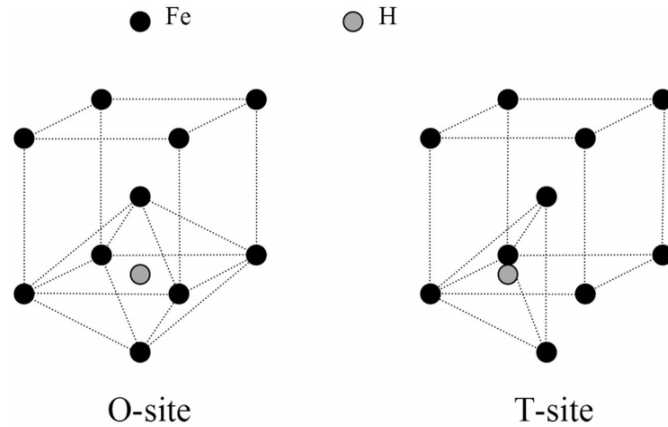


Figure 5. Shows preferred locations of hydrogen in the lattice.

Hydrogen can be easily absorbed in environments brought on by electroplating, pickling, casting, corrosion, fuel cell reactions, and even cathodic protection. The process in which hydrogen is absorbed into the metal is called hydrogen charging. The mechanism that allows charging to happen is the negatively charged current which carries the positively charged hydrogen ions into the metal. [12]

3.1.1. Effects of Electroplating Process on Hydrogen Pick-up

The process used to apply the coating may have an important effect on the properties of the entire coating system. One of the more important considerations is the effect of hydrogen formation during electroplating. Hydrogen may embrittle the substrate. This is particularly important when cadmium, chromium, or zinc is used as a coating over high-strength steel. Atomic hydrogen can combine to form high-pressure hydrogen gas at defects or regions of poor adhesion, causing blisters in the coating. Hydrogen can also be introduced into the coating system during one of the cleaning or pickling steps conducted before electroplating. [11] The source of hydrogen in all of these processes is the solution, whether it is the electrolyte for plating or the acid for cleaning processes. This is due to the fact that these solutions are water based. Unless the components are heat treated to release the absorbed hydrogen, they will be too brittle to utilize in any application that involves elastic strain. [4]

Of all the commonly plated metals, cadmium deposited from a cyanide solution is more likely to produce hydrogen embrittlement. To counteract the hydrogen pick-up of cadmium plating,

Boeing uses cadmium-titanium. Prior research on cadmium-titanium plating has shown the addition of titanium prevents hydrogen pick-up. Figure 6 shows that the increasing content of titanium in a non-cyanide solution decreases the hydrogen penetration current. The use of a non-cyanide electrolyte solution allows the titanium compound to be more stable. Cadmium-titanium plating is the current process used for plating high-strength landing gear parts due to the reduced hydrogen pick-up.

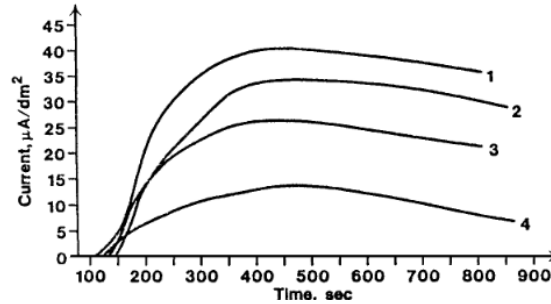


Figure 6. Hydrogen penetration current versus time in a non-cyanide electrolyte solution for cadmium plating with varying titanium concentrations: (1) no Ti, (2) 0.067 g/l Ti, (3) 2.2 g/l Ti, (4) 3.1 g/l Ti. [13]

A prior study was performed on the effects of the delay time between electroplating and hydrogen relief bake as well as the hydrogen relief baking time. Hydrogen relief bake time was observed for two extremes, 3 and 72 hours, while bake delay was observed for 0.25 and 24 hours. Table I shows that hydrogen relief bake time produced a large decrease in hydrogen concentration while bake delay time had little to no effect on hydrogen content. Despite the bake delay showing little effect on hydrogen concentration, the length of delay time could be sufficient enough that the hydrogen can reach critical concentration, which leads to crack initiation and no amount of hydrogen relief baking will repair these cracks.

Table I. Hydrogen Concentration Analysis of Cadmium Plated 4340 Steel with Varying Hydrogen Relief Bake and Bake Delay Times

| Trial | Baking Time (hr) | Bake Delay (hr) | Hydrogen Concentration ($\mu\text{A}/\text{cm}^2$) |
|--------------|-------------------------|------------------------|--|
| 1 | 3 | 0.25 | 1.07 |
| 2 | 3 | 24 | 1.05 |
| 3 | 72 | 0.25 | 0.28 |
| 4 | 72 | 24 | 0.30 |

3.1.2. Effects of Shot Peening Process on Hydrogen Pick-up

Generally speaking shot peening is assumed to reduce the permeability of ferritic steels to hydrogen. The reason is that compressive stresses on the surface produced by the shot peening prevent hydrogen atoms from permeating through, however few details are available to account for this beneficial effect. Furthermore, there is no clear relationship between shot peening and hydrogen pick-up, and this is because hydrogen pick-up depends on the material at hand and the hydrogen environment. For example, in heavy hydrogen environments like H_2S , shot peening of low carbon steel has shown to be detrimental in that more hydrogen is picked up. Also, for 304 stainless steel, shot peening increases hydrogen content and provokes hydrogen embrittlement. These examples show that shot peening can be counterintuitive in terms of its effects on hydrogen pick-up. [14]

4. Effects of Hydrogen Pick-up on 4340M High-strength Steel

4.1. Hydrogen Embrittlement

Hydrogen degrades metallic materials by cracking, blistering, hydride formation, decarburization, and lowers both tensile strength and ductility. High strength steel is susceptible to even small amounts of hydrogen pick-up. The two most relevant types of hydrogen embrittlement for landing gear are loss of ductility and hydrogen stress cracking. Loss of ductility in high-strength alloys can be combated by relieving the applied stress and aging at room temperature, if microcracks have not already formed. [15]

Hydrogen stress cracking is defined by the brittle fracture of an alloy due to hydrogen exposure. It is a mechanism for subcritical crack growth that produces time delayed fracture, and this can happen without an externally applied stress. Hydrogen moves to areas of high tensile stress, so notches are especially susceptible to fracture. Because this is a diffusion-controlled process, slow sustained stresses are the biggest concern over impacts. Hydrogen stress cracking can also be called static fatigue, sustained-load cracking, or hydrogen-induced delayed fracture, due to the nature of hydrogen pick-up. [15]

Hydrogen cracking typically occurs in steels with a strength greater than 180 ksi, although it can also occur in weaker steels that have been heavily cold worked. The factors that influence the likelihood of cracking include the hardness or strength level, stress level, the duration of the sustained load, and the concentration of hydrogen. Ambient temperature is where cracking is most common, and it becomes less common with higher temperature. It is essentially non-existent after 390°F due to decreased stress levels. [15]

Crack branching can occur in hydrogen embrittlement, but it is less common than in stress corrosion cracking. For high-strength steels like 4340, the path is typically intergranular. However, transgranular cleavage has also been observed. [15]

4.2. Failure Modes

One of the most favorable properties of alloys is that they exhibit ductile failures. With ductile failure the material will plastically deform, and cracks will propagate only when more stress is applied to the material. On the other hand, when materials experience brittle failure they experience little to no plastic deformation, and cracks will propagate uncontrollably with no additional stress applied. Brittle failures can be catastrophic because they happen without warning.

There are essentially two fracture paths that are encountered in engineering alloys: transgranular fracture and intergranular fracture. Transgranular fracture occurs when the strength of the slip plane is weaker than the grain boundaries. This condition is more common at low temperatures. The typical path of transgranular fracture follows along the slip planes, which can be located anywhere within the grains. On the other hand, intergranular fracture has a path that follows the

grain boundaries. However, there are usually small amounts of transgranular fracture paths in most intergranular fractures. [16] A comparison of the two brittle fractures can be seen in Figure 7. [17]

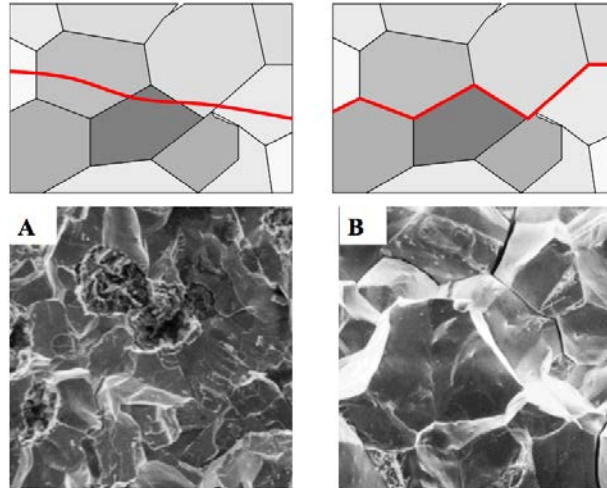


Figure 7. The illustration and micrograph on the left represent transgranular fracture. On the right are examples of intergranular fracture.

Hydrogen embrittled, high-strength alloys most often experience brittle intergranular fracture. Absorbed hydrogen has the tendency of diffusing to grain boundaries, where it bonds to form hydrides, weakening the original bonds between grains. Additionally, when hydrogen ions bond to form hydrogen gas, they put tremendous pressure on the lattice. Figure 8 is an example of intergranular fracture of cadmium plated 8740 steel caused by hydrogen embrittlement. [15]

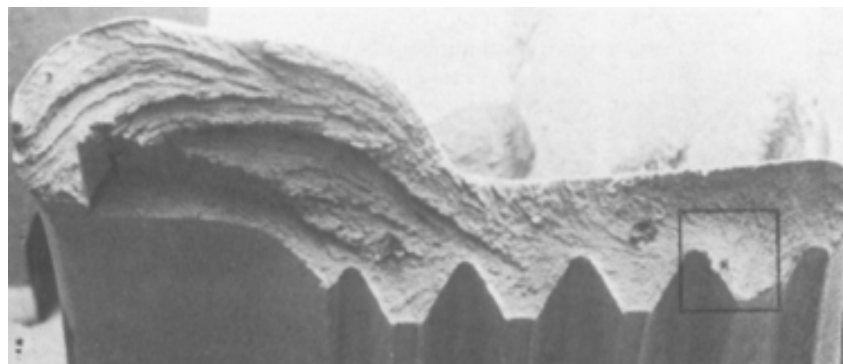


Figure 8. Brittle failure of cadmium plated steel nut.

The most common failure mode for hydrogen embrittled engineering alloys is decohesive rupture. This type of rupture occurs when the material exhibits little plastic deformation before failure and does not occur by dimple rupture, cleavage, or fatigue. The reason why this mode is

so common is because it generally results from a reactive environment or a unique microstructure and is associated almost exclusively with rupture along grain boundaries. Grain boundaries are easy paths for diffusion and sites for the segregation of such elements as hydrogen, sulfur, phosphorus, arsenic, and carbon. The presence of these constituents at the boundaries can significantly reduce the cohesive strength of the material at the boundaries and promote decohesive rupture. [18]

Additionally, continuous stress is a problem for high-strength steel with absorbed hydrogen because the hydrogen moves to areas of high stress concentrations, such as notches. It is for this reason that notched tensile tests are used to test samples where hydrogen embrittlement may be an issue. In these tests, samples are held at a constant tensile stress for up to a week to allow the hydrogen to move through the sample. [19]

4.3. Hydrogen Relief Bake

Hydrogen relief bakes are a necessary part of processing for electroplated 4340M steel because hydrogen is an inevitable side effect of electroplating. Hydrogen relief bakes use heat provide the structure with enough kinetic energy to let the hydrogen ions (H^+) escape from a lower energy state (preferential sites) to the outside of the steel. The bakes are time sensitive because the longer the hydrogen stays in the steel, the more likely it will bond to other atoms. When H^+ bonds to itself, it turns into a molecule of hydrogen gas which has a much harder time diffusing out of the lattice during a bake. The molecule also increases stress in the lattice which can contribute to brittle failure. Hydrogen ions in the steel can develop hydrides and degrade the bonds in the grain boundaries. In both of these situations, damage to the steel is permanent if the hydrogen relief bake is not performed. [15]

When hydrogen absorption happens, both reversible and irreversible damage can occur. It is important to remove the hydrogen from the alloy before the damage becomes irreversible. Because hydrogen pick-up is an inevitable part of electroplating, Boeing specifies a maximum amount of time between electroplating and hydrogen relief baking for their alloys. These specifications are summarized in Table II. The nut in Figure 8 fractured as a result of an improper hydrogen relief bake where the sample was not baked for long enough. [15]

Table II. Boeing Specifications for Hydrogen Relief Baking of Chromium, Nickel, and Cadmium-Titanium 300M Steel at a Bake Temperature of 375°F [7] [20] [21]

| Electroplating Type | Maximum Bake Delay | Minimum Bake Delay |
|----------------------------|---------------------------|---------------------------|
| Cadmium-Titanium | 8 hours | 12 hours |
| Chromium | 10 hours | 12 hours |
| Nickel | 10 hours | 23 hours |

4.4. Stress Relief Bake

Different types of materials can retain residual stresses, especially when they have a complex shape and have to go through intricate processes. Components with small section sizes, for example, are more sensitive to stresses because the processes that the parts have to go through to produce those sections are more involved. However, as section size becomes relatively uniform and large throughout, the impact of the stresses is lower. [22]

Residual stresses reduce the material's resistance to crack initiation, which makes processing and dimensional changes more difficult. Dimensional changes affect the component mainly if the residual stress in a body is eliminated. This allows dislocations introduced by residual stresses in the part to relocate to a lower stress state or even dissipate, altering its shape. Tensile residual stresses, in addition, promote crack initiation, and cracks have a highly detrimental effect on the tensile properties of the material. [23] Additionally, heat-treated steels, particularly those plated and used at 35 HRC and above, are susceptible to hydrogen embrittlement. Most susceptible is spring steel that has not been adequately stress relieved after forming. [8]

Causes of residual stresses are all related to variations in stresses, temperatures, and chemical species within the body during the processes that the material goes through. Examples of processes that induce residual stress are forming, machining, heat treatment, shot peening, casting, welding, flame cutting, and plating. These render their characteristic residual stress pattern to processed parts. [17]

In heat-treated parts, for example, residual stresses are caused by a thermal gradient alone. The thermal gradient produces a structural change like a phase transformation, which impacts the

strains and stresses within the body of the part. Quenching steel from the austenitizing temperature to room temperature is an example of the high stresses that can be induced through thermal gradients. When the steel is quenched, carbon is trapped within the lattice given that does not have enough time to diffuse out, so the lattice strain is extremely high, and the internal stress of the material structure is tremendously increased.

Stress relief baking is a technique utilized to relieve those residual stresses. The principle or mechanism involved in stress relieve baking is similar to the concept of creep. In creep, dislocations (microscopic defects) rearrange in response to the heat of the annealing process. The temperature rises, so dislocations obtain sufficient energy to move to a lower energy state or are obliterated. As dislocations move to a lower energy state, the component becomes stress relieved or relaxed. This condition will reduce hardness and strength, but only by a small amount. The main idea is to relieve the residual stresses within the component without losing the desired properties of the part. [22]

Furthermore, stress-relief temperatures are not high enough to be detrimental to the desired material. After this relaxation (dislocations moving to a lower energy states) has occurred, the component is cooled to room temperature slowly and with enough uniformity that it will not produce a high enough temperature gradient to induce residual stresses. Residual stresses can never be fully eliminated, but the degree to which the material will become stress relieved depends mainly on the initial severity of the residual stresses, the stress-relieving temperature and time at temperature, the heating/cooling cycle, and the chemistry and metallurgical structure of the material. [22]

5. Experimental Procedure

5.1. Safety

Safety was always the first priority for every aspect of this project. The Cal Poly materials engineering department has specific safety protocol required for all laboratory procedures. In all laboratory spaces, safety glasses, long pants, and close toed shoes were worn. Laboratory work was always performed with a minimum of two team members present. During the notching of

the panel coupons for lab fractures, a face shield was used to prevent injury from flying sparks and debris. Also, electroplating debris would fly off the sample during tensile testing, so a plexiglass shield was placed in front of the Instron testing system for protection.

5.2. Samples

There were three sample types that were utilized in the project. These were the flat panel specimens, the rotating beam fatigue specimens, and the notched tensile specimens. These underwent different processes and tests that will be discussed further in this section.

5.2.1. Sample Types

Table III describes the types of samples in more detail and includes the processing that the samples went through. There were a total of 18 flat panel specimens of which nine were shot peened and nine were not. Of these nine, there were three samples for each plating which corresponded to a bake delay specification. The “no bake” condition meant that the sample was not baked, the “specified bake” condition corresponded to samples that had been baked under standard conditions according to Boeing’s specifications, and the “delayed bake” had been baked, however, the bake delay was longer than that of the threshold specified in Boeing’s standards.

Table III. Sample Types and Processing Specifications

| Type of Sample | Surface Treatment | Electroplating Type | Bake Delay Specification |
|-------------------------|------------------------|----------------------|--------------------------|
| Flat Panel Specimens | Non-shot Peened (4340) | Nickel (3) | No Bake |
| | | | Delayed Bake |
| | | | Specified Bake |
| | | Chromium (3) | No Bake |
| | | | Delayed Bake |
| | | | Specified Bake |
| | Cadmium-Titanium (3) | No Bake | |
| | | Delayed Bake | |
| | | Specified Bake | |
| Shot Peened (4340M) | Nickel (3) | No Bake | |
| | | Delayed Bake | |
| | | Specified Bake | |
| | Chromium (3) | No Bake | |
| | | Delayed Bake | |
| | | Specified Bake | |
| Cadmium-Titanium (3) | No Bake | | |
| | Delayed Bake | | |
| | Specified Bake | | |
| Notched Tensile Samples | Non-Shot Peened (4340) | Nickel (2) | No Bake |
| | | Chromium (2) | Specified Bake |
| | | Cadmium-Titanium (2) | No Bake |
| Rotating Beam Specimens | Shot Peened (4330M) | Nickel (2) | Specified Bake |
| | | | No Bake |
| | | Chromium (2) | Specified Bake |
| | | | No Bake |
| | | Cadmium-Titanium (2) | Specified Bake |
| | | | No Bake |

5.2.2. Material Variation

There is some variation in the material that the different sample types were made out of even though they are all high-strength, low alloy steels. The non-shot peened flat panels and the notched tensile samples were 4340 steel, the shot peened panels were 4340M steel, and the rotating beam specimens were made out of 4330M steel. The difference between the 4340 steel and the 4340M steel is that the 4340 steel is air melted and contains inclusions due to the processing of the alloy. The 4340M steel is vacuum arc melted instead, which reduces the amount of impurities brought into the material during the process. The strength for both the 4340 and the 4340M steel ranges from 275 ksi to 300 ksi. The 4330M steel is also vacuum arc melted providing a low inclusion count, however its strength ranges only from 200 ksi to 220 ksi.

5.2.3. Sample Preparation

We cut a large, shot peened, 4340M flat panel into eight coupons using an abrasive saw, and then repeated the process for a non-shot peened 4340 panel. The eight non-shot peened panel coupons were then put into an oven for a stress relief bake. All sixteen coupons were sent to Boeing, where a nital etch inspection was performed to check for potential burns caused by the abrasive saw. All of the coupons passed.

5.3. Sample Processing

This section provides information on the specific processes that the material went through before the testing portion of the project was started. Specific information about the processing steps is needed to be able to understand the results in depth.

5.3.1. Shot Peening

Shot peening was applied to half of the samples in accordance with BAC 5730 (Boeing's Shot Peening Standard). This specification explains the depth of the compressive layer through the force utilized in the process, as well as the type of shot media utilized and the time the sample was peened for. For the most part both of these parameters varied according to the electroplating type and the alloy. However, typically the shot peening media is made of a ceramic composite of alumina, zirconia, and silica. The force and time that the sample is subjected to shot peening depends on the size of the sample along with the desired depth of the compressive layer.

5.3.2. Electroplating

For this investigation into the effects of electroplating on hydrogen embrittlement, three types of electroplating were performed across the various sample types: chromium, nickel, and cadmium-titanium. Chromium plating was applied in accordance with BAC5709 (Class 3) with a thickness of 0.010" to 0.015". Nickel plating was applied in accordance with BAC5746 (Type III) to a thickness of 0.010" to 0.012". Cadmium-titanium was plated in accordance with BAC5804 to a thickness of 0.001" to 0.002". The electroplating thicknesses were consistent across the three sample types (flat panels, rotating beam, and notch tensile).

5.3.3. Hydrogen Relief Bake

After the samples were electroplated, a hydrogen relief bake was performed on specimens that required either a bake within the specified time or an extended bake delay (Table IV, Table V). A third of the samples were not hydrogen relief baked to demonstrate the full effects of hydrogen picked up during electroplating. Boeing hydrogen relief bake specifications are summarized in Table IV. It should be noted that the cadmium-titanium specified bake has a bake delay that is 16 hours longer than Boeing Specification (8 hours). This is due to an error by the plating company. All “delayed bake” samples had a one week bake delay to give an insight to the time sensitivity of hydrogen relief bakes.

Table IV. Bake Delay Times for Notched Tensile Specimens and Fatigue Coupons

| Sample | Bake Delay |
|--------|------------|
| Cd-SB | 1 day |
| Cd-NB | N/A |
| Cr-SB | 1.5 hours |
| Cr-NB | N/A |
| Ni-SB | 0.5 hours |
| NI-NB | N/A |

Table V. Bake Delay Times for Panel Specimens

| Sample | Bake Delay |
|--------|------------|
| Cd-SB | 1 days |
| Cd-DB | 7 days |
| Cd-NB | N/A |
| Cr-SB | 1.5 hours |
| Cr-NB | 7 days |
| Cr-NB | N/A |
| Ni-SB | 0.5 hours |
| Ni-DB | 7 days |
| NI-NB | N/A |

5.4. Metallography

Boeing facilities provided metallography samples of the three different plating types that had already been mounted, polished, and etched. Each sample was imaged through optical microscopy at 100x and/or 200x magnitude to capture the structure of the plating types. The electroplating structures were used to determine the relative hydrogen relief bake efficiencies between the various plating types.

5.5. Testing

The testing for this project included investigation of mechanical properties and fracture behavior, which will be described further in this section. The rotating beam specimens and notch tensile specimens were tensile tested and the panel specimens were manually fractured. The fracture surfaces of all specimens were analyzed using the scanning electron microscope.

5.5.1. Tensile Testing

Both the notched tensile samples and rotating beam specimens were tensile tested utilizing standard tensile testing procedures. Since we could not apply a sustained load test for the notched tensile samples, and the rotating beam specimens are not meant to be tensile tested, no specific standard could be utilized. The testing was only done to compare qualitatively between sample groups, not necessarily to obtain a quantitative value for the failure load or ultimate tensile strength.

For the notched tensile samples, a button head fixture was ordered and utilized to hold the samples fixed in the Instron tensile testing machine grips. The crosshead displacement rate utilized was relatively low (0.1 in./min.), which allowed the hydrogen to propagate to preferential sites and show its effects on the material. Figure 9 shows the test setup for the notched tensile samples. The maximum stress (σ_{max}) was calculated based on the smallest diameter at the notch and the load at failure. This calculation is performed utilizing Equation 1.

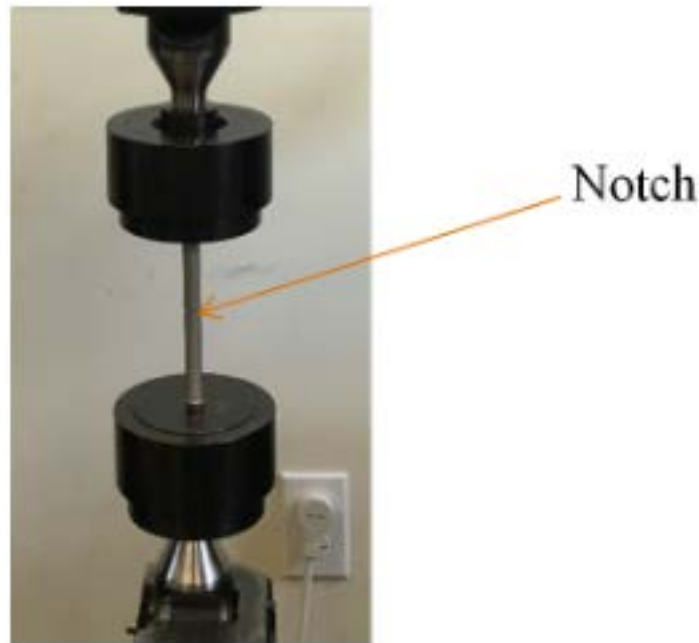


Figure 9. The test setup for the notched tensile samples is shown. The samples were inserted in the button head fixtures and pulled at a rate of 0.1 in./min.

$$\sigma_{max} = \frac{P_{Max}}{A_{Notch}} \quad (1)$$

The rotating beam fatigue specimens were also tensile tested. These were subjected to a crosshead displacement rate of 0.2 in./min. The samples were fixed in V-grips in order to prevent them from slipping from the grips during the test. The maximum load was obtained from the load frame and maximum strength (σ_{max}) was calculated from the smallest diameter in the sample (Equation 2). In addition, percent reduction of area was calculated by measuring diameters before and after testing. Figure 10 shows one of the samples after testing. Note that they were then utilized for scanning electron microscopy, so the surfaces were carefully handled.

$$\sigma_{max} = \frac{P_{failure}}{A_{smallest}} \quad (2)$$



Figure 10. Rotating beam specimen after tensile test is shown. Note that the sample was tested at a crosshead rate of 0.2 in./min.

5.5.2. Laboratory Fractures

Flat panel specimens were cut out with a cold-cut saw into rectangular flat panels with dimensions of 1.5 in. x 0.5 in. x 0.25 in. (Figure 11). They were notched to about one third of the thickness using a dremel with an abrasive saw, placed in a vise where they were fixed and manually fractured with a breaker bar. The fracture surfaces were then observed, imaged, and failure modes were characterized.

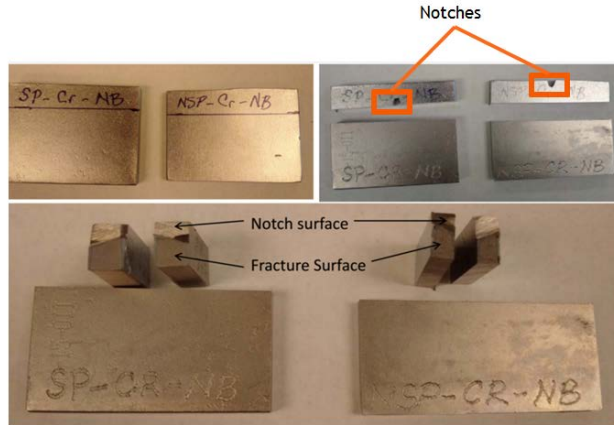


Figure 11. This image shows the flat panel specimens that were cut out into the lab fracture samples, the notches, and the final sample surfaces. The samples used for the lab fractures had dimensions of roughly 1.5 in. x 0.5 in. x 0.25 in.

5.6. Fracture Surface Analysis

After the samples had been properly cleaned with acetone, they were mounted on a standard aluminum scanning electron microscopy pin stub, to which the samples were taped utilizing a conductive graphite tape. Standard operating procedures were utilized to take images of the fracture surfaces of the steel samples. Most of the images were taken beneath the surface near the outer edge of the steel close to the electroplating. This is because the compressive stresses induced by shot peening on the steel change to tensile stresses at about one tenth of an inch in depth. Since the hydrogen tends to propagate to areas of tensile stress, and enters the component through the outside layer, it finds preferential sites near the edge of the surface first. Thus, the most embrittled regions would appear in these zones. Furthermore, images of the embrittled areas were taken at 500x, 1000x, and 2500x magnification in order to be able to characterize the failure modes, and distinguish between brittle and ductile regions.

6. Results

6.1. Residual Stress Measurements

For the purposes of determining the effects of shot peening, residual stress measurements were performed on the surface of the flat panel specimens prior to and after shot peening. The residual stress plots in Figures 12 and 13 show the residual stresses with increasing depth into the surface of the sample. Two non-shot peened, flat panel specimens (Figure 12) reveal primarily positive

values that correlate to tensile stresses at the surface of the material. Within 0.004 inches into the depth of the sample, small compressive (negative) stresses are observed that were caused by abrasive blasting during surface preparation.

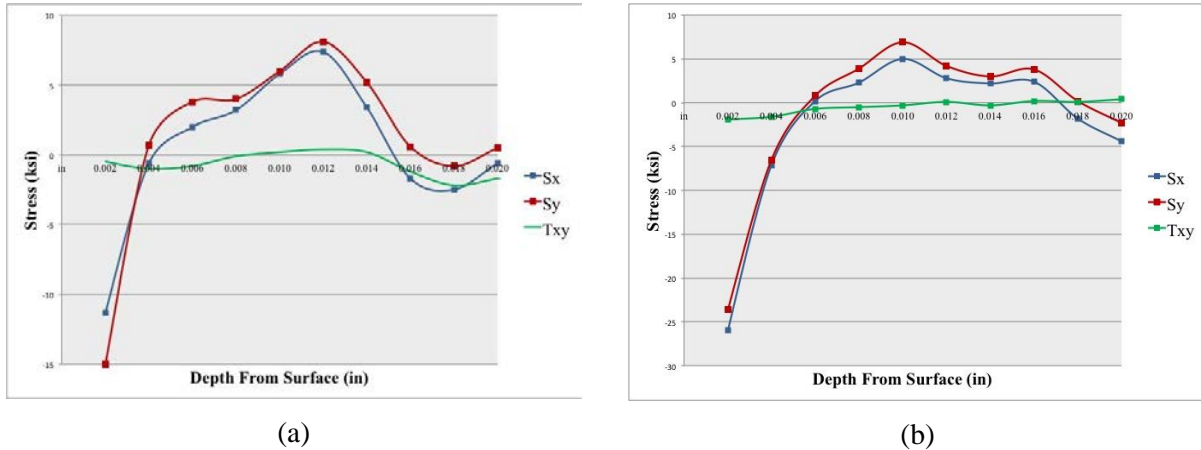


Figure 12. Residual stress plots for two non-shot peened, flat panel specimens demonstrating primarily tensile (positive) stresses near the surface with small compressive (negative) stresses up to 0.004" (a) and 0.005" (b) into the surface due to abrasive blasting.

Two shot peened, flat panel specimens (Figure 13), show large compressive (negative) stresses up to 120 ksi on the surface of the steel samples. As the depth into the surface increases, the compressive stresses decrease and change to tensile stresses around a depth of 0.012 inches. The magnitude and depth of the compressive stresses in the shot peened samples is significantly greater compared to the compressive stresses seen in the non-shot peened samples. This difference in compressive stress magnitude between the two conditions was considered significant enough for the purpose of studying the effects of shot peening versus non-shot peening with hydrogen pick-up.

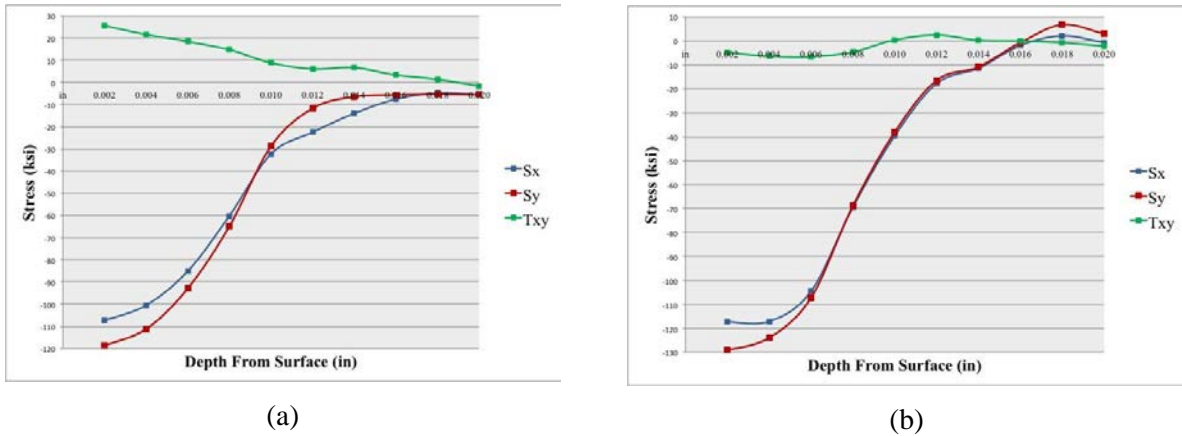


Figure 13. Residual stress plots for two shot peened, flat panel specimens demonstrating primarily compressive (negative) stresses up to 0.012" (a) and 0.005" (b) into the surface due to shot peening.

6.2. Metallography

Different types of electroplatings have different microstructures, and these are important to understand in order to be able to discuss the baking efficiency of the materials. Figure 14 shows the microstructures of the three platings at a 100x magnification (Ni) and 200x magnification (Cr and Cd-Ti). Notice that the Cd-Ti microstructure is highly porous, as compared to the Ni plating, which is compact and dense. The Cr plating is compact and dense, however it suffers from microcracking which can be seen through the dark river-like patterns in the plating.



Figure 14. These images show the microstructures of the three platings. Notice the porosity of the Cd-Ti plating, and the density and compactness of the Ni and Cr ones. In addition, the note that the Cr plating suffers from microcracking.

6.3. Hydrogen Relief

The porous microstructure of cadmium-titanium provides paths for hydrogen to diffuse out of the material, resulting in a high baking efficiency. The nickel plating's compact and dense microstructure, on the other hand, makes hydrogen relief less efficient. The microcracks in the chromium plating provide a pathway for hydrogen to escape that is comparable to that of cadmium-titanium. Table VI reinforces this idea, where for each shot peening specification paired with an electroplating type, the hydrogen measurement from the "no bake" condition was subtracted from the hydrogen measurement of the "specified bake" condition. This results in the amount of hydrogen released during the hydrogen relief bake, providing a measure for baking efficiency.

Table VI. Bake Out Efficiency

| Sample | Normalized Hydrogen Relief |
|---------------|-----------------------------------|
| NSP-CD | 2 |
| SP-CD | 3.75 |
| NSP-CR | 3.75 |
| SP-CR | 2.75 |
| NSP-NI | 2.5 |
| SP-NI | 1 |

6.4. Hydrogen Pick-up

Table VII shows the effect that shot peening has on H pick-up. The hydrogen content of two samples (one shot peened and one non-shot peened) was measured at two stages in the processing line for a chromium plated sample. The hydrogen content of the "as received" condition, which had not been plated, and the content of the same sample after it had been Cr

plated was quantified. The difference between these is the H picked-up during the electroplating process. Notice that the H pick-up is higher for the non-shot peened sample than the shot peened one. This lead us to conclude that shot peening, in fact, reduces H pick-up.

Table VII. Shot Peening Effects on Hydrogen Pick-up

| Specimen | Specification | Average Hydrogen Content (ppm) |
|------------------------|----------------------|--------------------------------|
| Non-Shot Peened | As Received | 0.85 |
| | Chromium Plated (NB) | 1.56 |
| | H Pick-up | 0.71 |
| Shot Peened | As Received | 0.57 |
| | Chromium Plated (NB) | 1.0 |
| | H Pick-up | 0.43 |

Table VIII shows the normalized hydrogen content for the flat panel specimens. Hydrogen measurements were taken for both the shot peened and non-shot peened samples for all the bake delay specifications. The actual H content (in ppm) was normalized to the lowest value of the measurements, given that the data is proprietary. Notice that the hydrogen content is higher for the non-shot peened samples of the same electroplating and bake delay specification all across the board. In addition, it can be clearly seen that as the bake delay increases the hydrogen content of the component increases. There is really no clear correlation between electroplating and the amount of hydrogen content.

Table VIII. Normalized Hydrogen Content for the Flat Panel Specimens

| Specimen | Normalized Hydrogen Content | Specimen | Normalized Hydrogen Content |
|-----------------|------------------------------------|-----------------|------------------------------------|
| NSP-CD-SB | 2 | SP-CD-SB | 1 |
| NSP-CD-DB | 3 | SP-CD-DB | 1.75 |
| NSP-CD-NB | 4 | SP-CD-NB | 4.75 |
| NSP-CR-SB | 3 | SP-CR-SB | 2.25 |
| NSP-CR-DB | 3.25 | SP-CR-DB | 2.5 |
| NSP-CR-NB | 7.8 | SP-CR-NB | 5.0 |
| NSP-NI-SB | 3.5 | SP-NI-SB | 2.5 |
| NSP-NI-DB | 4.25 | SP-NI-DB | 3 |
| NSP-NI-NB | 6 | SP-NI-NB | 3.5 |

Figure 15 displays the correlation between the hydrogen relief bake specifications and hydrogen pick-up. The bar chart shows that as bake delay increases, hydrogen pick-up increases as well.

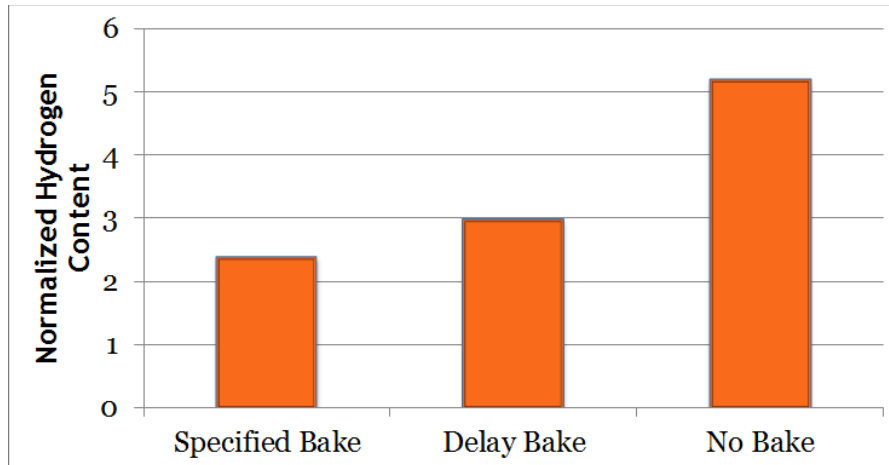


Figure 15. This bar chart further shows the effects of the hydrogen relief bake delay specifications on the hydrogen content of the sample. Note that as bake delay increases, hydrogen pick-up increases.

6.5. Tensile Testing Results

The tensile results for the rotating beam specimens are seen in Table IX. The table shows the failure load, the diameter before testing, the maximum stress, and percent reduction of area. Notice that the base average (non-plated sample) has the highest maximum stress. In addition, there is a significant difference in maximum stress between the baked samples and the ones that were not baked. Figures 16 and 17 further exemplify these effects.

Table IX. Mechanical Properties of Rotating Beam Fatigue Specimens

| Sample | Failure Load (kip) | Diameter Before (in) | Maximum Stress (ksi) | %RA |
|-----------|--------------------|----------------------|----------------------|-------|
| Base Avg. | 7.87 | 0.215 | 216.70 | 29.09 |
| SP-Cd-SB | 7.83 | 0.219 | 215.78 | 25.96 |
| SP-Cd-NB | 7.73 | 0.216 | 212.97 | 27.55 |
| SP-Cr-SB | 7.84 | 0.246 | 215.95 | 14.33 |
| SP-Cr-NB | 7.63 | 0.249 | 210.23 | 12.60 |
| SP-Ni-SB | 7.79 | 0.246 | 214.45 | 38.21 |
| SP-Ni-SB | 7.64 | 0.244 | 210.33 | 36.74 |

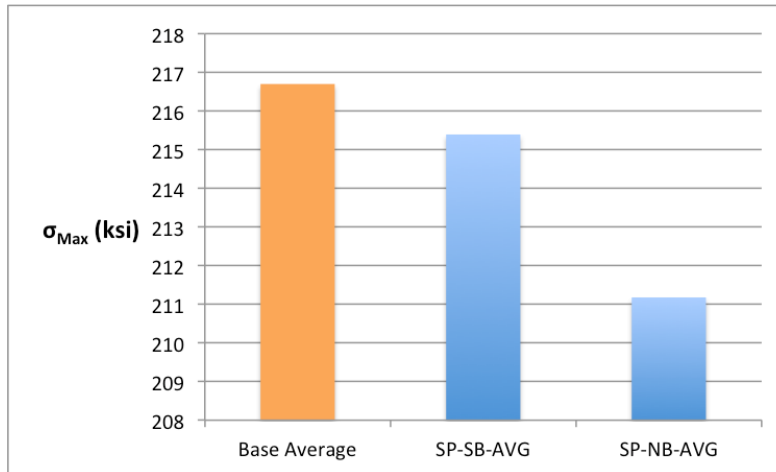


Figure 16. This figure shows the average maximum stresses of the samples in the “as received” condition (baseline), the shot peened samples in the “specified bake” condition, and the shot peened samples in the “no bake” condition. These are the rotating fatigue beam specimens which means that the material is 4330M steel in the 200-220 ksi range. This figure shows the fact that electroplating does in fact embrittle the material, lowering σ_{max} . In addition, there is a significant difference between samples that are baked, and samples that are not, where the baked samples have a much higher maximum stress.

The failure loads of the notched tensile samples are shown in Table X together with the diameter of the notch and the maximum stress calculated. The load at fracture was obtained through the Instron tensile testing machine, the diameter of the notch was retrieved from the mechanical drawing in the machining specification of the sample, and the maximum stress was calculated through the diameter of the notch.

Table X. Mechanical Properties of Notched Tensile Samples

| Sample | Diameter (in) | Failure Load (kip) | Maximum Stress (ksi) |
|-----------|---------------|--------------------|----------------------|
| Baseline | 0.2355 | 16.65 | 382.67 |
| NSP-Cd-SB | 0.235 | 15.22 | 350.85 |
| NSP-Cd-NB | 0.235 | 16.14 | 372.05 |
| NSP-Cr-SB | 0.235 | 15.74 | 362.98 |
| NSP-Cr-NB | 0.235 | 5.29 | 122.02 |
| NSP-Ni-SB | 0.235 | 16.46 | 379.59 |
| NSP-Ni-NB | 0.235 | 16.1 | 371.18 |

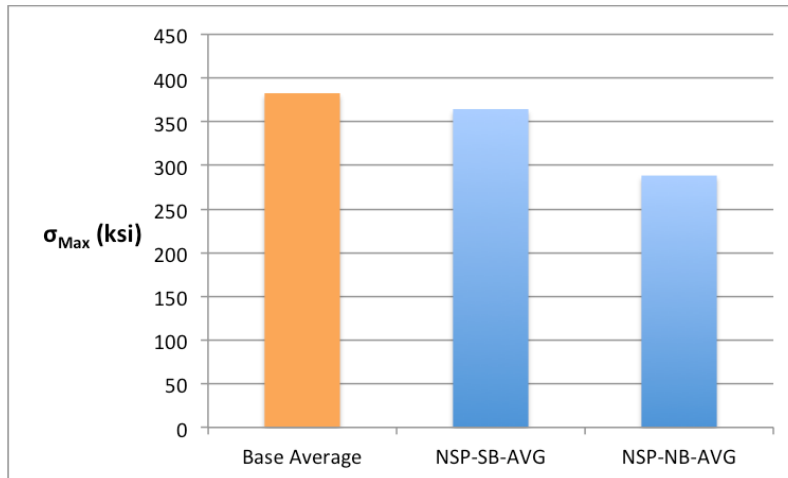


Figure 17. This figure shows the average maximum stresses of the samples in the “as received” condition (baseline), the non-shot peened samples in the “specified bake” condition, and the non-shot peened samples in the “no bake” condition. These are the notched tensile samples which means that the material is 4340 steel in the 275-300 ksi strength range. The stress concentration factor of the notch was not included in the calculations, however a relative comparison of the values is still valid. Notice that electroplating does in fact embrittle the material, lowering σ_{max} . In addition, there is a significant difference between samples that are baked, and samples that are not, where the baked samples have a much higher maximum stress.

6.6. Fracture Analysis

The SEM fractographs taken for the non-shot peened panels are shown in Figures 18-20; for the shot peened panels, the fracture surfaces are shown in Figures 21-23. All fracture surfaces show a mixed mode of brittle and ductile fracture. The brittle regions are characterized as brittle facets (transgranular cleavage), whereas the ductile regions display ductile dimple rupture. Notice that as bake delay increases the samples display a higher amount of brittle fracture regions. In addition, note the fact that the shot peened samples show more ductile features than the non-shot peened ones.

6.6.1. Non-shot Peened Flat Panels

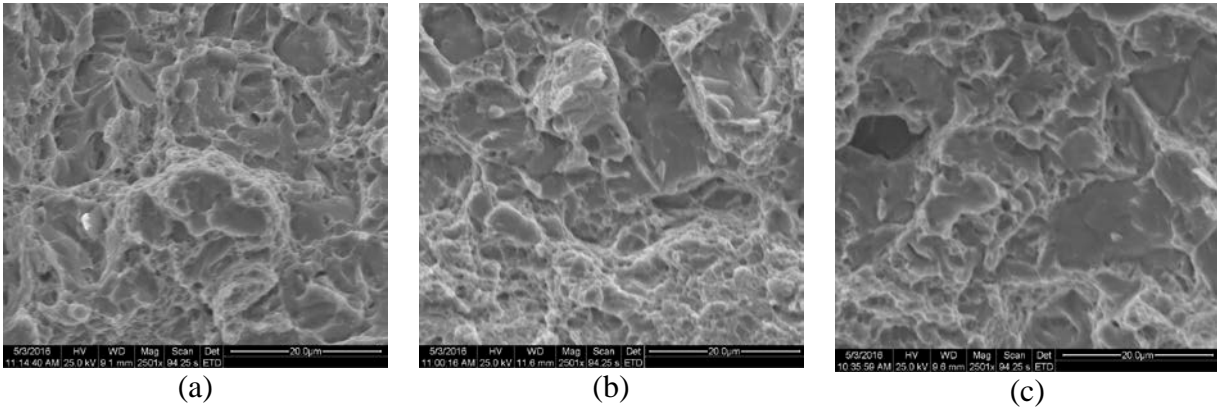


Figure 18. Scanning electron microscope fractographs (2500x magnification) of non-shot peened, nickel panel specimens with increasing bake delay: (a) specified bake (b) delayed bake (c) no bake. As bake delay increase, the prominence of brittle facets increases and the ductile dimple regions decrease.

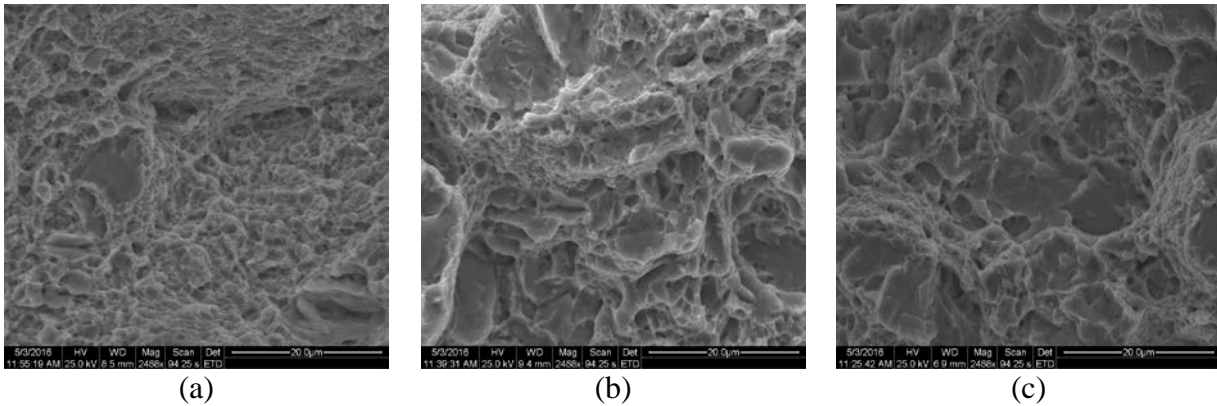


Figure 19. Scanning electron microscope fractographs (2500x magnification) of non-shot peened, hard chromium panel specimens with increasing bake delay: (a) specified bake (b) delayed bake (c) no bake. As bake delay increase, the prominence of brittle facets increases and the ductile dimple regions decrease.

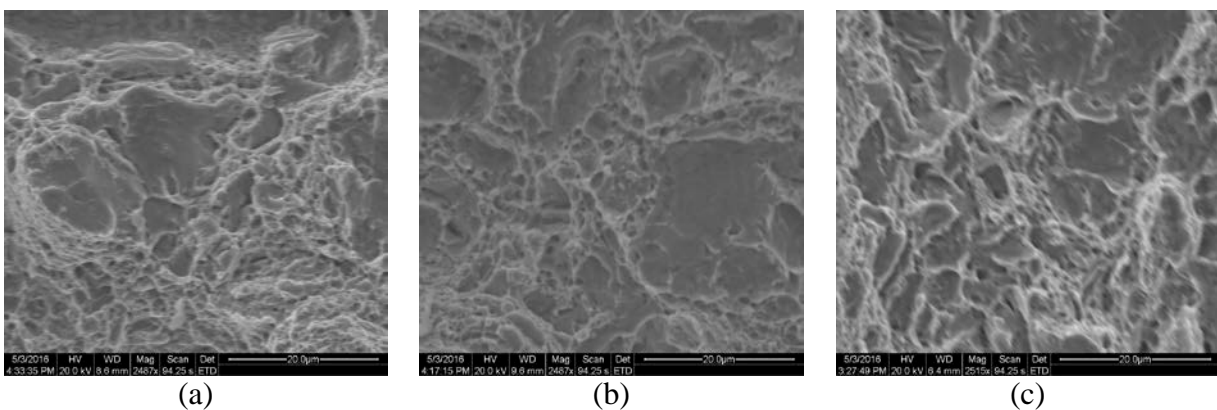


Figure 20. Scanning electron microscope fractographs (2500x magnification) of non-shot peened, cadmium-titanium panel specimens with increasing bake delay: (a) specified bake (b) delayed bake (c) no bake. As bake delay increase, the prominence of brittle facets increases and the ductile dimple regions decrease.

6.6.2. Shot Peened Flat Panels

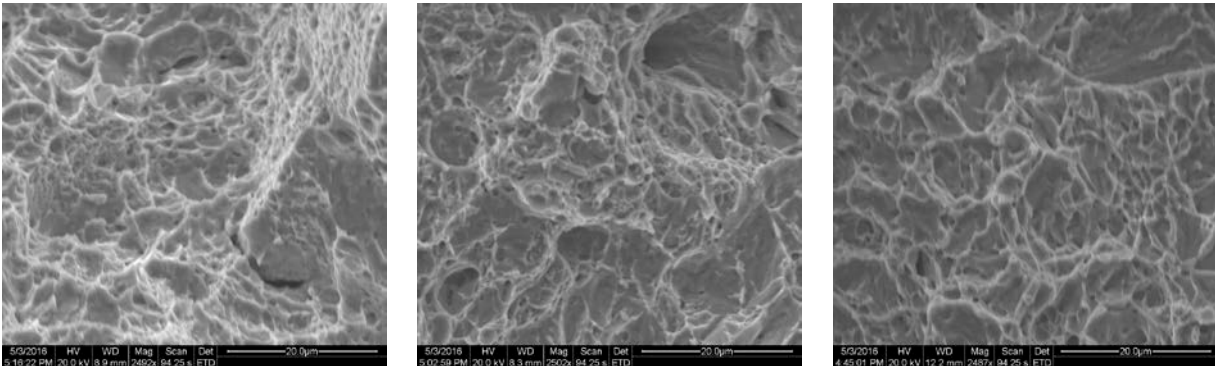


Figure 21. Scanning electron microscope fractographs (2500x magnification) of shot peened, nickel panel specimens with increasing bake delay: (a) specified bake (b) delayed bake (c) no bake. All the images appear to be primarily ductile but as bake delay increase, the prominence of brittle facets increases and the ductile dimple regions decrease.

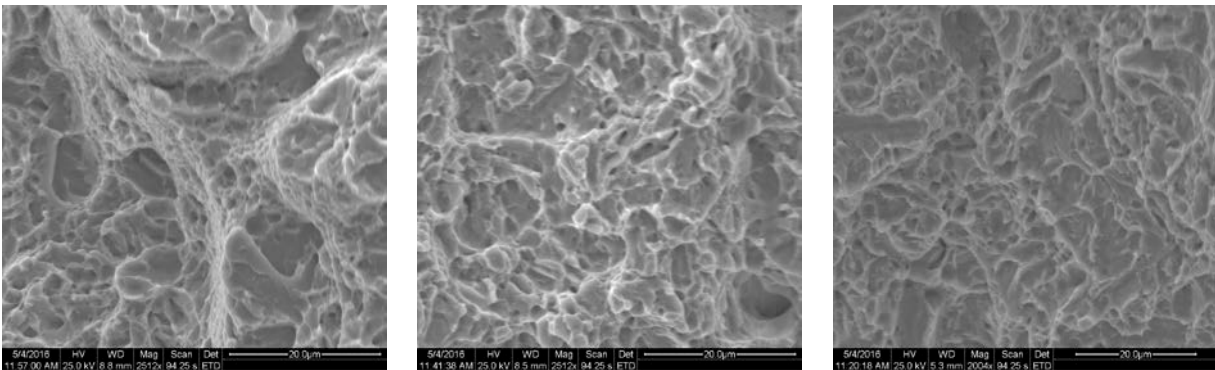


Figure 22. Scanning electron microscope fractographs (2500x magnification) of shot peened, hard chromium panel specimens with increasing bake delay: (a) specified bake (b) delayed bake (c) no bake. All the images appear to be primarily ductile but as bake delay increase, the prominence of brittle facets increases and the ductile dimple regions decrease.

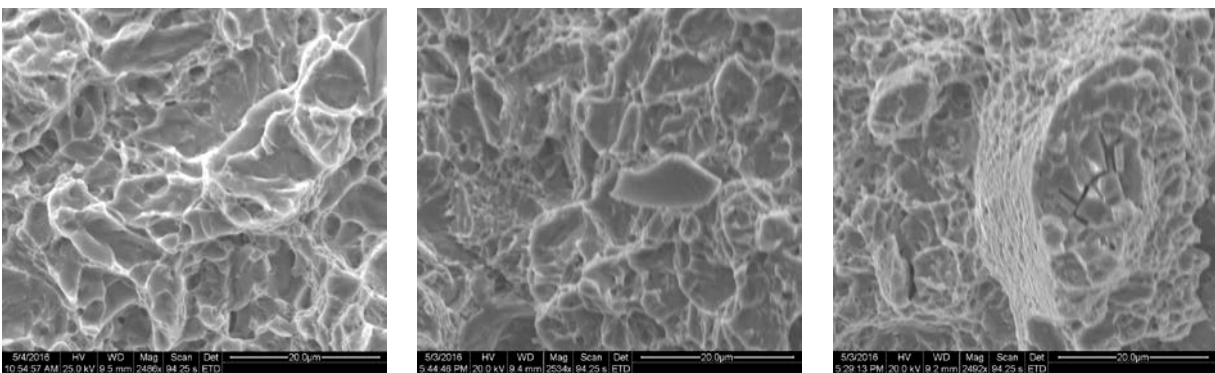


Figure 23. Scanning electron microscope fractographs (2500x magnification) of shot peened, hard chromium panel specimens with increasing bake delay: (a) specified bake (b) delayed bake (c) no bake. All the images appear to be primarily ductile but as bake delay increase, the prominence of brittle facets increases and the ductile dimple regions decrease.

7. Discussion

7.1. Baking Efficiency

It was expected that the porous cadmium-titanium plating would outperform both nickel and chromium in terms of baking efficiency. This was true in the case of the nickel plating, which had an average normalized hydrogen relief of 1.75, compared to the cadmium-titanium average normalized hydrogen relief of 2.88. However, cadmium-titanium with a measurement of 2.88 did slightly worse than chromium with a 3.25 value. The porous cadmium-titanium was expected to be a better pathway for hydrogen diffusion compared to the dense and compact structure of the chromium plating which contained microcracks. Also the chromium plating was significantly thicker than the cadmium-titanium making the effect more pronounced. This leads to the conclusion that the microcracks in the chromium plating structure are a better diffusion path for hydrogen than the pores in the cadmium-titanium electroplating.

7.2. Effect of Shot Peening on Hydrogen Pick-up

The purpose of shot peening landing gear components is to improve fatigue life by increasing resistance to crack propagation. In addition, it turns out that the surface stresses induced by shot peening reduce hydrogen diffusion into the material during the electroplating process. This can be seen in Table VII, where hydrogen content of a shot peened and a non-shot peened sample was measured in the 'as received' condition and after the Cr plating had been applied. The hydrogen pick-up was determined to be the difference between the Cr plated sample and the sample in the 'as received' condition. The H pick-up was higher for the non-shot peened sample than it was for the shot peened one, which lead us to believe that shot peening reduces hydrogen pick-up. This phenomenon occurred across all plating types. Other studies have shown this same effect where they demonstrate the suppression of the permeation of hydrogen due to the compressive residual stress at the surface [24]. Little research has been done as to why this occurs, but it seems that the compression of the bonds between atoms prevents hydrogen diffusion.

7.3. Effect of Bake Delay on Hydrogen Pick-up

The delay before a hydrogen relief bake was one of the primary focuses since it could be readily controlled as opposed to electroplating, which has the unfortunate side effect of hydrogen pick-up. The normalized hydrogen content for the flat panel specimens and their various processing parameters are shown in Table VIII and the averages for the three bake delays are shown in Figure 15. From Figure 15, the specimens that had a hydrogen relief bake performed within the specified bake delay time had the lowest average hydrogen content. As bake delay increases, the hydrogen content in the steel also increases. This phenomenon results as hydrogen is allowed more time to diffuse to preferential sites in the lattice structure, as well as recombine with other hydrogen atoms to form molecular hydrogen. Hydrogen is allowed enough time to diffuse to a lower energy state, requiring a higher amount of energy to bake it out. If the hydrogen relief bake does not provide sufficient activation energy to bake out hydrogen while in the molecular state or in preferred lattice sites which exist at lower energy states, more hydrogen will remain in the material. As a result, the panel specimens that had no hydrogen relief bake performed on them showed the greatest hydrogen content.

7.4. Effect of Bake Delay on Hydrogen Embrittlement

Increasing bake delay results in higher hydrogen content within the samples, given that hydrogen is allowed for more time to diffuse into its interstitial preferential sites before being baked. This allows the hydrogen atoms to bond with surrounding elements and form hydrides weakening bonds around it, or bond to itself forming hydrogen gas which puts high pressure on the lattice resulting in a material that is more brittle. This phenomenon reduces both the ductility and the tensile strength of the material, which was consistent with the data acquired. The fractographs taken through the scanning electron microscope of samples with varying bake delays displayed a mixed mode of ductile and brittle features. The brittle features were represented by cleavage facets, whereas the ductile features were characterized by ductile dimples. The relative amounts of brittle features, however, increased as bake delay increased. This effect is exemplified in Figures 18-20.

7.5. Effect of Electroplating on Hydrogen Embrittlement

One unfortunate side effect of electroplating is hydrogen pick-up. This phenomenon ultimately leads to embrittlement of the part when a proper hydrogen relief bake is not performed. Figures 16 and 17 show the average maximum tensile stresses for the rotating beam and notched tensile specimens. The baseline averages for both specimen types, which were not electroplated, showed the highest maximum tensile stresses. The samples in the 'no bake' condition had a significant decrease in tensile stress due to the large increase in hydrogen content from electroplating. The samples in the specified bake condition also showed a decrease in tensile stress as a result of electroplating. The hydrogen relief bake performed within the specified delay time reduced the embrittling effects to a minimal level.

8. Conclusions

1. The compressive surface layer induced by shot peening reduces hydrogen pick-up.
2. Electroplating reduces the maximum tensile stress of the steel via hydrogen embrittlement, however a proper hydrogen relief bake helps mitigate this effect.
3. As bake delay increases, both hydrogen pick-up and embrittlement increase.
4. Laboratory fractures are a valid empirical assessment of hydrogen embrittlement.

9. References

- [1] Aircraft Landing Gear Systems." Aviation Maintenance Technician Handbook - Airframe (2012). Aircraft Handbooks & Manuals. Federal Aviation Administration.
- [2] Private Communication, Dickerson, C., Associate Technical Fellow – Metallurgy, Boeing, 10 Nov. 2015.
- [3] Shot Peening." Surface Technologies Divison. Curtiss-Wright, 2005. Web. 18 Nov. 2015.
- [4] Surface Engineering: Effects of Surface Treatments on Materials Performance, Vol 5, ASM Handbook, ASM International, 1994.
- [5] Davis, J. R., ed. Corrosion : Understanding the Basics. Materials Park, OH, USA: ASM International, 2000. ProQuest ebrary. Web. 27 January 201.
- [6] J.R. Davis, Surface Engineering of Carbon and Alloy Steels, Surface Engineering, Vol 5, ASM Handbook, ASM International, 1994, p 701–740.
- [7] BAC 5804, "Low Hydrogen Embrittlement Cadmium–Titanium Alloy Plating," Boeing Airplane Company, 2004.
- [8] M.F. Stevenson, Sr., Cadmium Plating, Surface Engineering, Vol 5, ASM Handbook, ASM International, 1994, p 215–226.
- [9] K.R. Newby, Industrial (Hard) Chromium Plating, Surface Engineering, Vol 5, ASM Handbook, ASM International, 1994, p 177–191.
- [10] G.A. Di Bari, Nickel Plating, Surface Engineering, Vol 5, ASM Handbook, ASM International, 1994, p 201–212.
- [11] Sanchez, J, S.F Lee, M.A Martin-Rengel, J Fulla, C Andrade, and J Ruiz-Hervías. "Measurement of Hydrogen and Embrittlement of High Strength Steels." Engineering Failure Analysis, 201.
- [12] T. Mooney, Electroplated Coatings, Corrosion: Fundamentals, Testing, and Protection, Vol 13A, ASM Handbook, ASM International, 2003, p 772–785.
- [13] "Hydrogen Embrittlement." Tel Aviv University. Web. <http://www.tau.ac.il/~chemlaba/Files/Electrodeposition/13208_02.pdf>.
- [14] Brass, Am, Chene, J, Anteri, G, Ovejergarcia, J, Castex, L. "Role of Shot-peening on Hydrogen Embrittlement of a Low-carbon Steel and a 304 Stainless-steel." Journal of Materials Science, 26.16 (1991): 4517-4526.
- [15] Hydrogen Damage and Embrittlement, Failure Analysis and Prevention, Vol 11, ASM Handbook, ASM International, 2002, p 809–822.
- [16] G.F. Vander Voort, Visual Examination and Light Microscopy, Fractography, Vol 12, ASM Handbook, ASM International, 1987, p 91–16.
- [17] "Introduction to Material Science: Failure." University of Virginia. Web. <<http://people.virginia.edu/~lz2n/mse209/Chapter8.pdf>>.
- [18] V. Kerlins and A. Phillips, Modes of Fracture, Fractography, Vol. 12, ASM Handbook, ASM International, 1987, p. 12–71.

- [19] ASTM F519-13, "Standard Test Method for Mechanical Hydrogen Embrittlement Evaluation of Plating/Coating Processes and Service Environments," ASTM International, West Conshohocken, PA, 2013.
- [20] BAC 5709, "Low Hydrogen Embrittlement Chromium Alloy Plating," Boeing Airplane Company, 2015.
- [21] BAC 5756, "Low Hydrogen Embrittlement Nickel Alloy Plating," Boeing Airplane Company, 2015.
- [22] J.L. Dossett and C.V. White, Introduction to Cast Iron Heat Treatment, Heat Treating of Irons and Steels. Vol 4D, ASM Handbook, ASM International, 2014, p 483–492.
- [23] A.K. Sinha, Defects and Distortion in Heat-Treated Parts, Heat Treating, Vol 4, ASM Handbook, ASM International, 1991, p 601–619.
- [24] A.K. Sinha, Defects and Distortion in Heat-Treated Parts, Heat Treating, Vol 4, ASM Handbook, ASM International, 1991, p 601–619.
- [25] ASTM A646/A646M, 2006, "Standard Specification for Premium Quality Alloy Steel Blooms and Billets for Aircraft and Aerospace Forgings," ASTM International, West Conshohocken, PA, 2011.
- [26] Mori, K, E Lee, W Frazier, K Niji, G Battel, A Tran, E Iriarte, O Perez, H Ruiz, T Choi, P Stoyanov, J Ogren, J Alrashaid, and O Es-Said. "Effect of Tempering and Baking on the Charpy Impact Energy of Hydrogen-Charged 4340 Steel." Journal of Materials.